The *Caenorhabditis elegans* IMPAS gene, *imp-2*, is essential for development and is functionally distinct from related presenilins

Anastasia P. Grigorenko*†‡, Yuri K. Moliaka*†, Martha C. Soto§, Craig C. Mello¶, and Evgeny I. Rogaev*†‖**

*Department of Psychiatry, Brudnick Neuropsychiatric Research Institute, University of Massachusetts Medical School, 303 Belmont Street, Worcester, MA 01604; †Laboratory of Molecular Brain Genetics, Research Center of Mental Health, Russian Academy of Medical Sciences, Zagorodnoe Shosse 2/2, Moscow 113152, Russia; ‡Institute of Molecular Genetics, Russian Academy of Sciences, Kurchatov Square 2, Moscow 123182, Russia; §Department of Pathology and Laboratory Medicine, University of Medicine and Dentistry of New Jersey–Robert Wood Johnson Medical School, 675 Hoes Lane, Piscataway, NJ 08854; ¶Program in Molecular Medicine, University of Massachusetts Medical School, Howard Hughes Medical Institute, 373 Plantation Street, Worcester, MA 01605; and ‖A. N. Belozersky Institute of Physical and Chemical Biology, Lomonosov Moscow State University, Moscow 119992, Russia

Communicated by S. J. Singer, University of California at San Diego, La Jolla, CA, September 2, 2004 (received for review June 25, 2004)

Presenilins (PSs) are required for Notch signaling in the development of vertebrates and invertebrates. Mutations in human PS1 and PS2 homologs are a cause of familial Alzheimer's disease (AD). The function of the recently identified ancient family of IMPAS proteins (IMP/SPP/PSH) homologous to PSs is not yet known. We show here that, unlike PSs, IMPs (orthologous *C. elegans Ce-imp-2* and human hIMP1/SPP) do not promote Notch (*C. elegans lin-12,glp-1*) proteolysis or signaling. The knock-down of *Ce-imp-2* leads to embryonic death and an abnormal molting phenotype in *Caenorhabditis elegans*. The molting defect induced by *Ce-imp-2* deficiency was mimicked by depleting cholesterol or disrupting *Ce-lrp-1* and suppressed, in part, by expression of the *Ce-lrp-1* derivate. *C. elegans lrp-1* is a homolog of mammalian megalin, lipoprotein receptor-related protein (LRP) receptors essential for cholesterol and lipoprotein endocytosis and signaling. These data suggest that IMPs are functionally distinct from related PSs and implicate IMPs as critical regulators of development that may potentially interact with the lipid-lipoprotein receptor-mediated pathway.

Presenilin 1 and presenilin 2 (PS1/*PSEN1* and PS2/*PSEN2*) were initially identified by positional cloning of the genes for Alzheimer's disease (AD) (1, 2). Mutations in human PS1 are a frequent cause of early-onset familial AD, and mutations in human PS2 underlie more rare early- or late-onset AD cases (1–3). Many tested missense- or deletion/insertion-AD mutations in PSs increase production of fibrillogenic Aβ42, presumably by means of γ-secretase cleavage of amyloid precursor protein (APP) membrane-tethered derivates. The data support the role of amyloid in the etiology of AD (4). Many lines of evidence show that human PS1 and PS2 and their homologs in other organisms (SEL-12 and HOP-1 in *Caenorhabditis elegans*) are unusual polytopic endoproteases capable of cleaving different type I transmembrane proteins within their membrane-spanning domains (5–8). The primary evolutionary conserved function of PSs in vertebrates and invertebrates is regulation of the Notch (*lin-12,glp-1* in *C. elegans*) signaling pathway during embryogenesis. Knock-out PS1 mice display a lethal phenotype similar to mice with Notch receptor and ligand knock-outs. Inactivation of both PS homologs *hop-1* and *sel-12* in *C. elegans* induces defects described for *lin-12* and *glp-1* loss-of-function mutants (9, 10). Moreover, the loss-of-function *sel-12* mutant suppresses multivulva phenotype in "hyperfunctional" *lin-12* mutants (11). The results demonstrate that PSs/*sel-12,hop-1* facilitate signaling by means of Notch/*lin-12,glp-1* receptors. Recently, genes encoding proteins homologous to PSs and termed IMPAS (or IMP/PSH/SPP,SPPL, hereafter referred to as IMPs) have been found (12–14, ††). The abundant ancient family of orthologous and paralogous IMP proteins is conserved from yeast to humans and share structural similarities with *Archaea* proteins and prokaryotic type 4 prepilin peptidases (TFPP) (15). The intramembrane proteolytic activity of human Impas 1 (hIMP1/SPP), an evolutionary conserved member of this protein family, has been shown. Direct examination in cultured cells or *in vitro* assays demonstrated that hIMP1/SPP is capable of cleaving hydrophobic signal peptide domains (14) or multipass-transmembrane protein substrates (15). The presumable intramembrane cleavage may release potentially bioactive short peptides or may be involved in maturation or trafficking of the proteins (16, 17). However, the *in vivo* functions of IMP proteins are as yet unknown. Here, we describe the analysis of *imp*-genes in *C. elegans* (*Ce-imp*). We show that *Ce-imp-2*, an ortholog of human hIMP1/SPP, is required for embryonic development and larval molting in *C. elegans* but is not required for Notch/(*lin-12,glp-1*) signaling and, therefore, has a function distinct from homologous presenilins. Instead, our data suggest that *Ce-imp-2* is involved in the cholesterol-lipoprotein receptor (Ch-LR)-dependent development pathway and raise the possibility that the mammalian ortholog, IMP1/SPP, may have similar function.

Materials and Methods

***C. elegans* Strains and Clones.** The following strains were used: N2 Bristol as a wild-type strain; *sel-12(ar131)*, *sel-12(ar131)unc-1*, *sel-12(ar171)unc-1 (e538)* (provided by I. Greenwald, Columbia University, New York), *glp-1(e2142ts)* (provided by C. Goutte, Amherst College, Amherst, MA), *lin-12(n137)/unc-32(e189)III;him-5(e1467)V*, *unc-32(e189)lin-12(n676n930)III*, *lrp-1(ku156)/gld-1(q266) I* (provided by the Caenorhabditis Genetics Center, which is funded by the National Institutes of Health National Center for Research Resources).

cDNA clones yk671a5, yk336d12, yk1191b02, and yk260f8 were obtained from Y. Kohara (Genome Biology Laboratory, National Institute of Genetics, Mishima, Japan). We used standard methods of *C. elegans* handling and culture (18) with OP50 *Escherichia coli* strain as a food source. Worms were observed by using a dissecting microscope with a maximum magnification of $\times$40–60 or a fluorescent dissecting stereo-microscope with a Nomarski optic and magnification of up to $\times$100. Filipin staining was performed as described (19).

Double-Stranded RNA (dsRNA) Synthesis and Injections. To generate dsRNA for injection, a T7 sequence was added at both ends of

Abbreviations: AD, Alzheimer's disease; ISC, incomplete shedding of cuticle; PS, presenilin; dsRNA, double-stranded RNA; RNAi, RNA interference; LRP, lipoprotein receptor-related protein.

**To whom correspondence should be addressed. E-mail: evgeny.rogaev@umassmed.edu.

††Rogaev, E. I., Grigorenko, A., Ryazanskaya, N., Sherbatich, T., Molyaka, Y., Korovaitseva, G. I. & Dvoryanchikov G. (2001) Sixth Human Genome Meeting, April 19–22, 2001, Edinburgh, **N101,** p. 28 (abstr.).

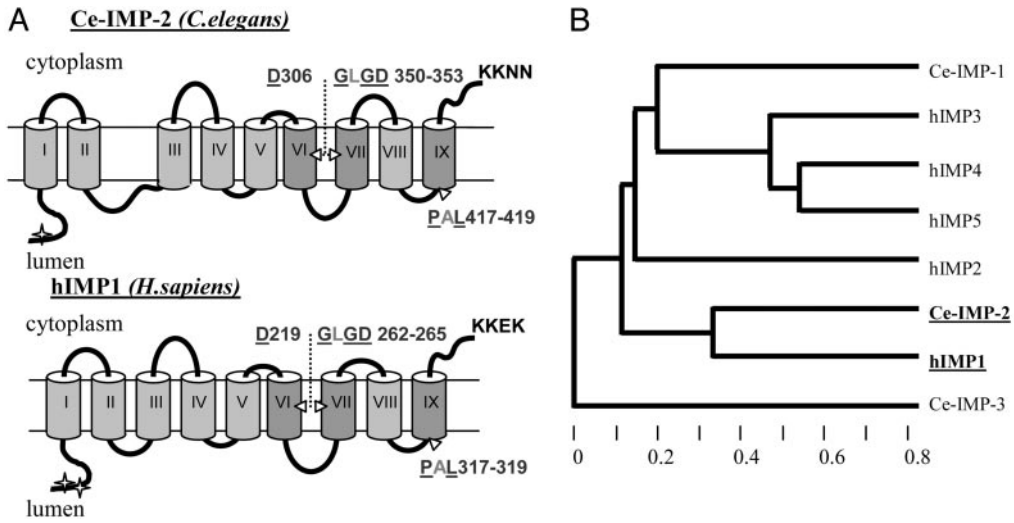

Fig. 1. Similarity of Ce-IMP-2 to other members of IMPAS and presenilin families of proteins. (*A*) Predicted transmembrane structure of Ce-IMP-2, *C. elegans*, and hIMP1, *Homo sapiens*. The arrowheads denote the positions of conserved aspartate and PAL-motif residues. The letters show invariant amino acid residues in eukaryotic PSs and IMPASes; the underlined letters are identical also in related proteins from *Archaea* and bacterial polytopic type 4 prepilin peptidases (TFPP). Most conserved domains in PSs and IMPAS families are shown in intense gray. The predicted sites of N-glycosylation (marked by asterisks) and endoplasmic reticulum-membrane retention signals (KKXX motif) are shown (NETNGLYC 1.0 and PSORT II predictions). (*B*) Phylogenic tree (Cluster algorithm, GENEBEE) for conserved domains (amino acid 269–444) of *C. elegans* Ce-IMP-2 and corresponding domains of *C. elegans* Ce-IMP-1, Ce-IMP-3, and human IMP (hIMP1–5) proteins.

the cDNA template by PCR reaction with corresponding primers. PCR product was then purified on Qiagen (Valencia, CA) columns and used for RNA synthesis and purification by using Ambion (Austin, TX) MEGAscript T7 Transcription Kit. RNA was then checked on standard agarose gel, was quantified ($\approx$ 1–5 μg/μl), and was used for pseudocoelomic injections [in head and tail regions beyond the positions of the two gonad arms (20, 21)] with an average of 0.5–1 $\times$ 10^6 RNA molecules per animal. Four to six hours after injection, worms were transferred individually to fresh plates, and the phenotype of F_1 progeny was analyzed within 2–3 days.

RNA Interference (RNAi) by dsRNA Feeding. RNAi by dsRNA feeding was performed as described (22–24). cDNAs for *C. elegans Ce-imp-1*, *Ce-imp-2*, and *Ce-imp-3* were cloned directly from yk clones or as PCR subfragments into an L4440 vector containing a double T7 promoter sequence (Fig. 5, which is published as supporting information on the PNAS web site).

Germ-Line Injections and Extrachromosomal Array. For *Ce-lrp-1* rescue experiments, germ-line injections of plasmid containing *Ce-lrp-1 L-ICD* were performed as described (25). *Ce-lrp-1L-ICD* fragment was cloned into *Bam*HI-*Pst*I L4440 vector. *Ce-lrp-1L-ICD* contains a 996-bp *Ce-lrp-1* promoter genomic region upstream of the ATG and a 1,026-bp 3′ genomic region downstream of stop codon TAA. Encoding sequence contains ICD fragment of *Ce-lrp-1* CDS with introduced ATG (5′-ATGGGACTTATTGGATTC) and ends on the last coding triplet of *Ce-lrp-1* CDS fused to myc-epitope sequence (Fig. 6, which is published as supporting information on the PNAS web site). DNA was injected in concentrations of 10–50 ng/μl into gonadal distal cells of young adult animals. The coinjection marker *sur-5-GFP* for easy detection of transgenic progeny was used in concentration at 10 ng/μl. Four to six hours after injection, the worms were transferred individually to fresh plates. To establish individual lines with extrachromosomal maintenance of the transgene, marker-positive F_1 animals were picked and placed separately.

Results

***Imp*-genes in *C. elegans*.** Multiple IMP/SPP-related genes were identified in a variety of species from yeast to human. At least five IMP genes in human and three diverged homologous genes similar to presenilins in *C. elegans* were identified. Comparison of the most conserved domains suggests links to a family of proteins in

Archaea and to bacterial peptidases (12, 15), indicating that *C. elegans* Ce-IMP-1, Ce-IMP-2, and Ce-IMP-3, like their human orthologs, may be polytopic proteases. The *C. elegans* Ce-IMP-1, Ce-IMP-2, and Ce-IMP-3 have divergent N termini but have substantial amino acid conservation in three hydrophobic regions predicted to be transmembrane (Tm) domains (Fig. 1; Fig. 7, which is published as supporting information on the PNAS web site). The amino acid signature 5DxxxV-LGxGD-PxL (where 5-F,Y,W; "x" is any amino acid, and "-" connects the three most conserved domains of the signature) is invariant in *C. elegans* Ce-IMP-1 and Ce-IMP-2 and members of IMPAS or PS families from distant taxons. Ce-IMP-3 is a more diverged family member, lacking this consensus signature but still harboring conserved aspartate and proline residues. The predicted Tm protein structure and membrane topology also resemble those described for human/*C. elegans* PS/SEL-12,HOP-1 proteins (Fig. 1*A*) (26, 27). Consistent with data for human IMP1/SPP, the sequences for endoplasmic reticulum retention signals were identified in the C-terminal part of Ce-IMP-2 and Ce-IMP-3, but not in Ce-IMP-1 (PSORT II prediction). The cluster algorithm and phylogenetic tree, limited to analysis of evolutionary conserved domains, demonstrate that Ce-IMP-2 has a more stringent homology to hIMP1/SPP than Ce-IMP-1 and Ce-IMP-3 (GENEBEE analysis, Fig. 1*B*). The percentage of identity/similarity for the entire amino acid sequence [hIMP1/Ce-IMP-1 (14/27); hIMP1/Ce-IMP-2 (30/46); hIMP1/Ce-IMP-3 (12/29)] also supports the idea that Ce-IMP-2 is an ortholog of hIMP1/SPP.

hIMP1 Does Not Promote S3-Cleavage of Notch1 in Mammalian Cells. Because PSs are major components of the protein complex regulating intramembrane Notch protein cleavage, we tested whether hIMP1/SPP, homologous to PSs, may also facilitate cleavage of the Notch1 receptor. Constructs with human IMP1 were generated that efficiently express hIMP1 in transiently and stably transfected mammalian cells. hIMP1 in cell lysates is

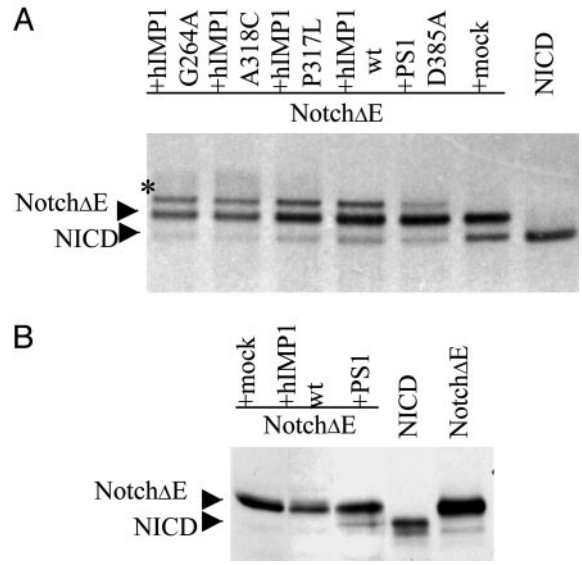

Fig. 2. Expression of human IMP1 in mammalian cells and S3 cleavage of Notch1 receptor. (*A*) Overexpression of hIMP1wt or mutant forms does not facilitate cleavage of Notch1 as detected by pulse–chase analysis. HEK293 cells were cotransfected with the constructs (*i*) NotchΔE and (*ii*) wild or mutant hIMP1 or PS1 D385A or mock (pcLacZ). NotchΔE and NOTCH1 intracellular domain (NICD) (predicted derivate of NotchΔ S3-cleavage) are fused to c-myc epitope. Cells were pulse-labeled and chased for 60 min. Protein extracts were immunoprecipitated with anti-c-myc antibodies and subjected to electrophoresis and autoradiography. As described, the NICD product of S3 cleavage is clearly detected in 60 min of pulse–chase in HEK293 cells expressing membrane-tethering NotchΔE. The coexpression of NotchΔE with loss-of-function PS1 D385A mutant has dominant-negative effect suppressing S3 activity of endogenous PS. The hIMP1wt or the hIMP1 mutant isoforms (G264A, A318C, and P317L) do not increase, but reduce efficiency of S3-cleavage. The modified Notch1 fragment observed in cells overexpressing IMP1 constructs is designated by asterisk. (*B*) Expression of hIMP1 in PS1$^{-/-}$,PS2$^{-/-}$ fibroblasts does not induce NotchΔE cleavage, unlike expression of exogenous PS1. Notch1 C-terminal fragments are detected by Western blot analysis with c-myc AB (Supporting information).

detected by Western blots in predicted 42- to 48-kDa and 95- to 98-kDa protein fractions. The high molecular mass 95- to 98-kDa fraction of exogenous or endogenous hIMP1 is likely homodimeric hIMP1 complex resistant to protein complex disassociation during protein extract preparation and SDS/PAGE procedures. However, upon expression of Ce-IMP-2 in HEK293 cells, only the predicted protein of molecular mass 50–55 kDa was dectected (Fig. 8*A*, which is published as supporting information on the PNAS web site, and refs. 12 and 28). PS1 was shown to be required for intramembranous S3 cleavage of NH_2-terminally truncated Notch derivates (NotchΔE) (6, 29). Mutations in the putative catalytic PS1 D257 and D385 residues inhibit proteolysis at the S3 site (30). We cotransfected HEK293 with NotchΔE (a substrate for intramembrane S3 cleavage) and hIMP1 or with the PS1 D385A construct, which inhibits the NotchΔE cleavage. The metabolic labeling and pulse–chase procedures demonstrated that hIMP1 does not induce or facilitate the NotchΔE S3 cleavage and generation of NOTCH1 intracellular domain (NICD) derivatives. Moreover, in cells overexpressing hIMP1, some inhibition of the NotchΔE S3 cleavage was detected comparable with the dominant negative effect of the PS1 D385A construct (Fig. 2*A* and Fig. 8 *B*, *C*, and *D*). Interestingly, a modified NotchΔE isoform was observed in cells overexpressing hIMP1. The wild-type and mutant IMP1 proteins had similar effects on modification of NotchΔE. The data demonstrate that hIMP1 does not facilitate NotchΔE S3 cleavage. In contrast to PS1wt, ectopic overexpression of hIMP1wt did not restore the S3 cleavage in PS1$^{-/-}$ PS2$^{-/-}$ mouse fibroblasts (Fig. 2*B*). Together, the data indicate that the substrate-dependent enzymatic function of hIMP1 is not redundant with PSs.

***Ce-imp-2* RNAi Does Not Affect *lin-12,glp-1* (Notch)-Signaling in Development in *C. elegans*.** To gain further insights into the possible functions of IMPAS genes *in vivo*, we used the *C. elegans* model. In our preliminary experiments, *Ce-imp-1* and *Ce-imp-3* dsRNAi produced no obvious development abnormalities. Therefore, we focused further upon study of *Ce-imp-2*, the ortholog of mammalian IMP1/SPP. Wild-type worms were injected with dsRNA or fed with *E. coli*-expressing dsRNA corresponding to the *Ce-imp-2* gene (Fig. 5). The search for the *sel-12*, *lin-12*, and *glp-1* characteristic phenotypes was performed over the course of multiple replicate experiments. There are several major defects caused by single or concomitant reduction of *lin-12* and *glp-1* (Notch homologs) and their upstream and downstream regulators. The first of these defects involves cell fate changes between the 4-cell and 12-cell stages that result in embryos lacking a portion of the pharynx and failing to enclose and elongate the body (31). Although the earliest defect caused by *Ce-imp-2* (RNAi) is embryonic arrest, <3% of *Ce-imp-2*(RNAi) embryos exhibited a failure to undergo body morphogenesis (Fig. 9*A*, which is published as supporting information on the PNAS web site). Instead, the majority of *Ce-imp-2* RNAi animals died during late embryonic stages or after hatching (Fig. 9 *B* and *C*). The lack of an anterior pharynx was previously described as a characteristic specific to diminished maternal *glp-1* activity, a decrease in the activity of factors required for *glp-1*,*lin-12* signaling (e.g., *sel-8*, *aph-1*, and *aph-2*) or the simultaneous reduction of *sel-12* and *hop-1* (9, 32, 33). We found that the development of anterior pharynx is normal in arrested larvae of *Ce-imp-2*-deficient N2 worms. Both Notch homologs *glp-1* and *lin-12* function together during late embryogenesis in the specification of the rectum (32). However, development of the rectum was unaffected in *Ce-imp-2*-deficient worms. Reduction of *Ce-imp-2* activity by RNAi did not induce defects in vulva formation similar to those described for mutants in *lin-12*/*Notch* or the *Ce-imp-2* homolog *sel-12* (10, 11, 32). Finally, we used sensitized genetic backgrounds to look for interactions between *Ce-imp-2* and Notch-pathway components. None of the hypo- or hypermorphic *glp-1*, *lin-12*, or *sel-12* mutant strains analyzed exhibited enhancement or suppression of their corresponding phenotypes upon induction *Ce-imp-2* (RNAi) (Fig. 3*A* and Table 1, which is published as supporting information on the PNAS web site). The data suggest that, unlike its distant homologs *sel-12* or *hop-1*, *Ce-imp-2* is not a positive regulator of *lin-12*,*glp-1* (Notch) signaling in cell–cell interaction and cell fate specification during development in *C. elegans*.

***Ce-imp-2* Inactivation Induces Embryonic Lethality and Molting Defects During Development.** Two major abnormalities induced by *Ce-imp-2* RNAi were embryonic/early L_1 lethality and L_1–L_4 larvae molting defects leading to larval arrest (Figs. 3*B* and 9 *A–G*). Studies of the progeny of adult worms injected with *Ce-imp-2* dsRNA showed 80–100% lethality of their offspring at late embryonic or early larval stages [number of experiments n = 7; total number of analyzed progeny n = 138 (100%); total number of dead worms on early stages 120 (87%)]. In an effort to avoid maternal germ-line effects and to delineate potential *Ce-imp-2* deficiency phenotypes in later development, we used RNAi by feeding.

Staged populations of L_1 worms were transferred to *Ce-imp-2* dsRNA plates and were analyzed for phenotypes in both initial generation (P_0 population) and their progeny (the F_1

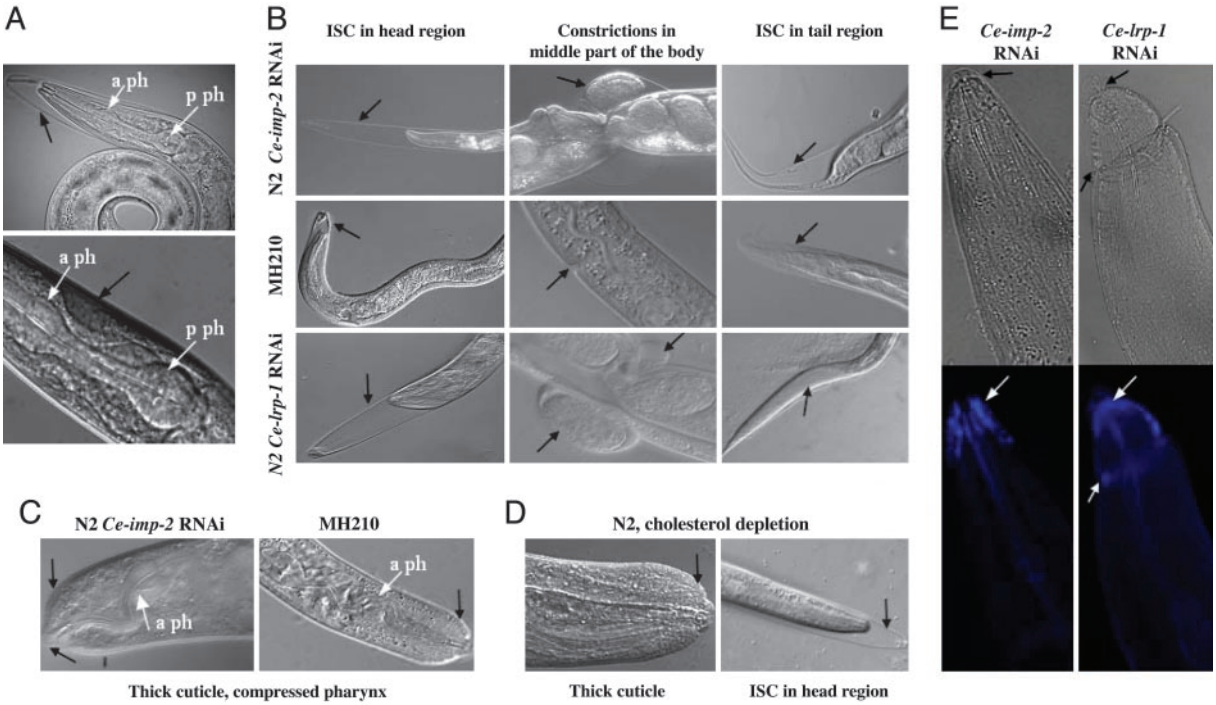

Fig. 3. Phenotypes induced by *Ce-imp-2* RNAi in *C. elegans* and cholesterol regulation-related pathway. Shown are Nomarski optic longitudinal views of *C. elegans* phenotypes. (*A Upper*) *Ce-imp-2* RNAi and *sel-12* reduced activities have no synergetic effects on *lin-12,glp-1* signaling. ISC defect induced by *Ce-imp-2* RNAi is observed in *sel-12 (ar131)* larvae, but pharyngeal anterior bulb is developed normally. (*A Lower*) Muscle detachment occasionally detected in N2 *Ce-imp-2* RNAi worms and normal pharyngeal anterior bulb are shown. (*B*) Similar ISC phenotypes are detected in *Ce-imp-2* RNAi N2 worms and in *Ce-lrp-1*-deficient worms (*Ce-lrp-1* RNAi N2 worms or *Ce-lrp-1* deletion strain MH210). (*C*) Thick cuticle and compressed pharynx in *Ce-imp-2* RNAi N2 and MH210 worms. (*D*) ISC phenotype and thick cuticle caused by cholesterol depletion in N2 worms. (*E*) Filipin complexes are localized in anterior head region in P_0 worms, which were fed with *Ce-imp-2* or *Ce-lrp-1* dsRNA (*Upper*, regular light, black arrows indicate ISC; *Lower*, UV-light picture, white arrows show filipin localization).

generation). Defects in P_0 development were observed at the L_3–L_4 and L_4-adult molt stages. At least 20–30% of N2 worms at these stages ($n = 9$; $n > 2 \times 10^3$) cannot properly shed the cuticle (Fig. 3*B*). In these cases, shedding of the cuticle was initiated, but the old cuticle remained attached to the body. Henceforth, we shall refer to this phenotype as the incomplete shedding of cuticle (ISC) phenotype. Analysis of individuals exhibiting this phenotype showed that ≈80% of these individuals failed to shed their cuticle and died, whereas the remaining 20% escape from the cuticle, which often remained attached to the tail region. These escapers matured to form sterile adults or Egl animals that could produce only a few eggs. The F_1 generation of the dsRNA Ce-IMP-2-fed animals exhibited phenotypes similar to those observed after microinjection of dsRNA. Approximately 3% of these embryos died at early stages before morphogenesis, whereas the majority died at late embryonic stages. Among the hatching F_1 progeny, the ISC phenotype was observed at all molt stages (Fig. 9 *D–G*). In experiments using F_1 embryos, we found that >60% of eggs died during late embryogenesis with elongated 3-fold embryos inside the egg shell or as early L_1 larvae, shortly after hatching ($n = 6, n > 10^3$). The remaining animals reached later stages, and most of them arrested with the ISC phenotype. Other postembryonic pathologies in *Ce-imp-2* RNAi worms included body constrictions (Fig. 3*B*), dumpy (Dpy), thick cuticle (Fig. 3*C*), exploded body (Rup, Fig. 9*J*), small body size (Sma), slow growth (Gro), slow pumping, uncoordinated movement (Unc), and muscle detachment (Fig. 3*A*).

Comparison of Phenotypes Caused by Depletion of *Ce-imp-2*, *Ce-lrp-1*, and Cholesterol. A similar ISC phenotype has been described for strains deprived of exogenous dietary cholesterol (34). However, this phenotype was not observed in another study in which cholesterol was completely removed from media (19). Recessive mutations in *C. elegans Ce-lrp-1* also result in defects in shedding the old cuticle during larval development (34). The *C. elegans* Ce-LRP-1 encoded by *Ce-lrp-1* is an epidermal protein homologous to mammalian low density lipoprotein receptors (LDLR), LRP1 (lipoprotein receptor related protein), and, in particular, megalin (termed also as LRP2/gp330). The LDLRs endocytose lipoproteins and regulate lipid homeostasis in mammals. We compared phenotypes caused by removal of supplementary cholesterol and by *Ce-imp-2* and *Ce-lrp-1* RNAi in parallel experiments. Under similar conditions, the *Ce-lrp-1* mutant MH210 [*lrp-1(ku156)/gld-1(q266)* strain] was also tested. Worms growing on plates with no supplementary cholesterol (as compared with standard plates with 5 μg/ml supplementary cholesterol) developed the ISC phenotype patterns similar to those found for *Ce-imp-2* RNAi animals (Fig. 3 *B–D*). As described in the original report (34), the ISC phenotype was not evident in F_1 but was displayed in successive generations after extended cultivation in cholesterol-free medium. Only a small amount of sterol is required for growth of insect cells and free-living nematodes (19, 35–37). Traces of cholesterol in agar, *E. coli*, or maternal supply in the eggs may be sufficient for normal development of F_1 (34), but not the following generations. We tested this prediction preparing ether-extracted peptone (19) for cholesterol-free agarose plates. As a result, we were able to detect 3.7% (75/2020) of animals with ISC in the P_0 generation in a synchronized population of worms. Many worms growing under these conditions remained small and weak. One possible model from our studies is that the *Ce-imp-2* is required for the production of a cholesterol-derived hormone important for molting. For example, the steroid hormone, 20-hydroxyecdys-

one, regulates molting in *Drosophila* (reviewed in ref. 38). However, these hormones have not yet been found in *C. elegans*.

We next compared phenotypes in *Ce-lrp-1* RNAi and *Ce-imp-2* RNAi worms. The effects of *Ce-lrp-1* RNAi were similar to *Ce-imp-2* RNAi, producing the ISC phenotypes during larval development. The partially detached cuticle found on all L_1–L_4 molt stages was seen frequently in the head and less frequently in the tail. Constrictions in the middle part of body were also found in both *Ce-lrp-1* and *Ce-imp-2* RNAi worms (Fig. 3*B* and Table 2, which is published as supporting information on the PNAS web site). The most noticeable difference was observed during the late embryonic/early L_1 stages; death was much less frequent or not detected in F_1 progeny of *Ce-lrp-1* RNAi-treated animals. Animals homozygous for *lrp-1(ku156)* showed the same ISC phenotypes observed in *Ce-lrp-1* (RNAi) (Fig. 3*B*). Arrested growth (with and without visual ISC), Unc, Sma, and occasional Dpy,Rup phenotypes were also identified in both *Ce-lrp-1*(RNAi) and *Ce-imp-2*(RNAi) animals. These effects may be related to the overly thick cuticle found in cholesterol-, *Ce-imp-2*-, and *Ce-lrp-1*-deficient worms (Fig. 3 *C* and *D*) and the inability to shed old cuticle compressing the growing body. The reduced brood size has been described in progeny of worms maintained on a reduced cholesterol diet (19, 39). We examined the brood size of individual worms on *Ce-imp-2* RNAi food. Worms that developed ISC at the L_4-adult stage died, some of them having a low number of progeny hatched inside dead mothers. The surviving worms were able to lay eggs over the next 2 or 3 days, but with a mean brood size at least 3-fold less than control RNAi worms (*Supporting Text*, which is published as supporting information on the PNAS web site). In summary, our data showed that *Ce-imp-2* deficiency phenotype resembles abnormalities induced by cholesterol depletion and closely mimics the *Ce-lrp-1* deficiency phenotype. Because *Ce-lrp-1* regulates endocytosis of cholesterol in mammals, it is conceivable that both *Ce-imp-2* and *Ce-lrp-1* may contribute to cholesterol uptake in *C. elegans*. Filipin is a fluorescent polyene antibiotic capable of forming complexes with cholesterol and other sterols in accumulation sites (19). Consistent with the idea that *Ce-imp-2* and *Ce-lrp-1* functions may contribute to cholesterol uptake or homeostasis pathway, filipin complexes accumulated in the body locations of *Ce-imp-2* RNAi animals where displacement of old cuticle normally is initiated (Fig. 3*E*).

The Cytoplasmic Terminus of Ce-LRP-1 Can Suppress the *Ce-imp-2* Defect Induced by RNAi. We tested further whether *Ce-imp-2* may be an upstream regulator of *Ce-lrp-1*- or *Ce-lrp-1*-dependent pathway in development. We asked whether the *Ce-imp-2* deficiency can be compensated by expression of Ce-LRP-1 protein derivate. The intracellular fragment of megalin contains FxNPxY and PxxPxxP conserved motifs essential for endocytosis and association with adaptor proteins (e.g., Ce-DAB-1) (Fig. 6). A construct encoding a cytoplasmic fragment of Ce-LRP-1 truncated in the N-transmembrane domain (*Ce-lrp-1 L-ICD*) was designed (Fig. 6 and *Supporting Materials and Methods*). The transgenic worm strains with extrachromosomal maintenance of *Ce-lrp-1 L-ICD* under *Ce-lrp-1* regulatory regions were generated. *Sur-5 GFP* plasmid was used as a coinjection marker. The wild-type N2 and strains with extrachromosomal maintenance of transgenic marker *sur-5 GFP* alone were used as controls. The synchronized population of worms at the L_1 stage were transferred to *Ce-imp-2* dsRNA plates, and, on day 3, worms were observed for the ISC phenotype as discussed above. The truncated *Ce-lrp-1* fragment caused profound rescue of the ISC defect caused by *Ce-imp-2* deficiency. This result was found and confirmed in two independent transgenic strains (Fig. 4). The rate of *Ce-imp-2* RNAi-induced ISC molting defect in *Ce-lrp-1* L-ICD strains was reduced 5- to 10-fold. These data suggest that *Ce-imp-2* may be directly involved in the regulation of Ce-LRP-1

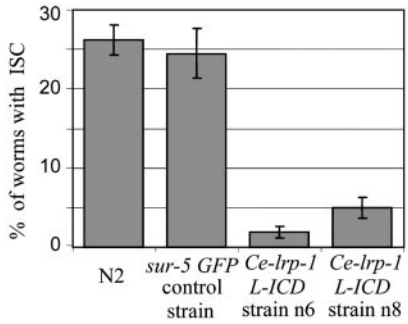

Fig. 4. Histogram showing compensatory effect of the NH_2-terminally truncated *Ce-lrp-1* fragment on the ISC defect caused by *Ce-imp-2* deficiency. Two independent transgenic strains (n6 and n8) with extrachromosomal maintenance of *Ce-lrp-1 L-ICD* construction and control N2 or *sur-5 GFP* control strains were analyzed. Synchronized strains on L_1 stage were placed on *Ce-imp-2* dsRNA plates, and P_0 worms with ISC phenotype were counted. There was significant reduction in ISC phenotype in *Ce-lrp-1 L-ICD* transgenic animals as compared with the controls ($P < 10^{-6}$, n = 2–4 independent trials, n = 1,262 and 1,084 for n6 and n8; n = 1932 and 707 for N2 and *sur-5 GFP* strains, correspondingly. Bar graphs represent the fractions and 95% confident intervals (CI) expressed in percentage of animals with ISC.

(by means of regulation of processing or trafficking) or may regulate other upstream elements interacting with the *Ce-lrp-1* pathway (Fig. 10, which is published as supporting information on the PNAS web site).

Discussion

Presenilins and IMPAS: Two Related Families of Proteins Regulating Distinct Development Pathways. We reported here a primary *in vivo* analysis of the functional role of the IMPAS (IMP) family of proteins, which are distinctly homologous to PSs. Both families (IMPs and PSs) share conserved amino acid signatures and structure identities thought to be critical for their intramembrane protease activities. Although a role of PSs in protein trafficking is also postulated, there are many arguments supporting the view that PSs and IMPs are unusual bi-aspartyl polytopic proteases with many structural and functional similarities. Moreover, many amino acid residues in PSs, which are targets for multiple mutations in AD, also occur and are evolutionary conserved in IMPs (15). Nevertheless, we demonstrate here that the Notch protein regulated by PSs is not a major target for the IMP proteins. *C. elegans Ce-imp-2* does not facilitate *sel-12*,*hop-1*-dependent *lin-12*,*glp-1* signaling. Our data, instead, indicated that IMPs and PSs are functionally distinct families of proteins regulating two different pathways in development. Phylogenic analysis demonstrated that IMPs have a more ancient ancestry prototype (found in *Archaea* and yeast) than PSs (found in *Protista*) (12). Thus, beyond the role of IMPs in the development of multicellular organisms, the common cellular functions of IMPs (e.g., in regulation of cell maintenance, proliferation, or cycles) remain be elucidated.

***Ce-imp-2*-Regulated Development Pathway.** *Ce-imp-2* is the ortholog of human IMP1/SPP, which is capable of cleaving or, at least, promoting the cleavage of some proteins within hydrophobic domains (14, 15, 17). The proteolytic properties of IMP1/SPP were demonstrated by direct assays *in vitro* and in cultured cells. The signal peptide peptidase activity of IMP1/SPP is thought to produce short peptide fragments that serve as HLA-E epitopes in mammals (16). However, the major function of human IMP1/SPP or their orthologs or paralogs remained to be uncovered.

The knock-down of *Ce-imp-2* performed herein revealed that *Ce-imp-2* is required for proper embryonic development and

completion of shedding of old cuticle in all four larval molts in *C. elegans*. A similar ISC phenotype was described for cholesterol-deficient worms. We noticed that loss-of-function in several other genes (*daf-9*,*nhr-23* and *nhr-25*,*Ce-lrp-1*,*let-512*,*dab-1*) has been described to result in abnormalities that include molting defects with ISC. Intriguingly, all of these genes seem to be involved in lipid steroid homeostasis or signaling. For example, the *C. elegans daf-9* gene regulates adult longevity and encodes a P450-cytochrome hydroxylase homologous to human CYP17 and CYP21 involved in biosynthesis of steroids (40). The dauer arrest found in *daf-9* mutants was not evident in *Ce-imp-2* RNAi worms. Thus, DAF-9 is unlikely to be the direct target regulated by *Ce-imp-2*. NHR-23 and NHR-25 are nuclear receptors, and NHR-25 is a homolog of mammalian FTZ-F1 receptor or FTZ-F1-like protein involved in regulation of cholesterol homeostasis (41–43). LET-512 is a member of the lipid kinase family that regulates localization and expression of Ce-LRP-1 in *C. elegans* (44). Ce-DAB-1 is related to a disabled family of cytoplasmic adaptor proteins interacting with LRPs and regulating the endocytosis of megalin and lipoprotein receptors in mammals. Recently, unshed cuticle molting defects induced by *Ce-dab-1* RNAi have been reported (45). Finally, Ce-LRP-1 is an ortholog of LRP-mammalian receptors and is suggested to be a close counterpart of megalin (34). One possibility is that Ce-IMP-2 promotes trafficking of Ce-LRP-1 to the cell surface. It is intriguing that expression of the cytoplasmic Ce-LRP-1 domain partially suppressed the molting defect induced by Ce-IMP-2 RNAi (Fig. 4). This finding suggests that signal transduction may be impaired in *Ce-imp-2* RNAi worms.

These observations illuminate the intriguing possibility that similar patterns of interacting molecules and pathways are involved in sterol homeostasis and cholesterol-lipoprotein receptor (Ch-LR)-dependent development in *C. elegans* and mammals. The ISC phenotype may be caused by partial deficiency in Ch-LR signaling and may serve as an excellent phenotype marker in the search for other molecular components of the *C. elegans* Ch-LR pathway. Known and yet unknown proteins interacting with the *Ce-lrp-1* pathway may be potential targets or downstream elements regulated by *Ce-imp-2* (Figs. 6 and 10). The role of *sel-12* in Notch-signaling is established (46). The *Ce-imp-2* controls distinct pathway. In summary, the data described here imply that Ce-IMP-2 and, perhaps, the human ortholog IMP1/SPP are essential regulators of development. Given the ancient origin and diversity of genes of the IMPAS family, their pleotropic functions are anticipated in both vertebrates and invertebrates

We thank members of our laboratories for technical assistance, Dr. I. Greenwald and Dr. C. Goutte for providing *C. elegans* mutant strains, Dr. Y. Kohara for providing *C. elegans* cDNA clones, Dr. R. Kopan (Washington University School of Medicine, St. Louis) for providing Notch1 constructs, and Dr. B. De Strooper (Center for Human Genetics, Katholieke Universiteit Leuven, and Flanders Interuniversity Institute for Biotechnology, Leuven, Belgium) for providing PS1 and PS2 knockout mouse fibroblasts. This work was supported by Alzheimer's Association Grant TLL-03-5777, and, in part, by the Howard Hughes Medical Institute, the Russian Foundation for Basic Research, and the National Institute of Neurological Disorders and Stroke.

1. Sherrington, R., Rogaev, E. I., Liang, Y., Rogaeva, E. A., Levesque, G., Ikeda, M., Chi, H., Lin, C., Li, G., Holman, K., *et al*. (1995) *Nature* **375,** 754–760.
2. Rogaev, E. I., Sherrington, R., Rogaeva, E. A., Levesque, G., Ikeda, M., Liang, Y., Chi, H., Lin, C., Holman, K., Tsuda, T., *et al*. (1995) *Nature* **376,** 775–778.
3. Levy-Lahad, E., Wasco, W., Poorkaj, P., Romano, D. M., Oshima, J., Pettingell, W. H., Yu, C. E., Jondro, P. D., Schmidt, S. D., Wang, K., *et al*. (1995) *Science* **269,** 973–977.
4. Hardy, J. & Selkoe, D. J. (2002) *Science* **297,** 353–356.
5. De Strooper, B., Saftig, P., Craessaerts, K., Vanderstichele, H., Guhde, G., Annaert, W., Von Figura, K. & Van Leuven, F. (1998) *Nature* **391,** 387–390.
6. De Strooper, B., Annaert, W., Cupers, P., Saftig, P., Craessaerts, K., Mumm, J. S., Schroeter, E. H., Schrijvers, V., Wolfe, M. S., Ray, W. J., *et al*. (1999) *Nature* **398,** 518–522.
7. Okochi, M., Eimer, S., Bottcher, A., Baumeister, R., Romig, H., Walter, J., Capell, A., Steiner, H. & Haass, C. (2000) *J. Biol. Chem*. **275,** 40925–40932.
8. Xia, W. & Wolfe, M. S. (2003) *J. Cell Sci*. **116,** 2839–2844.
9. Li, X. & Greenwald, I. (1997) *Proc. Natl. Acad. Sci. USA* **94,** 12204–12209.
10. Westlund, B., Parry, D., Clover, R., Basson, M. & Johnson, C. D. (1999) *Proc. Natl. Acad. Sci. USA* **96,** 2497–2502.
11. Levitan, D. & Greenwald, I. (1995) *Nature* **377,** 351–354.
12. Grigorenko, A. P., Moliaka, Y. K., Korovaitseva, G. I. & Rogaev, E. I. (2002) *Biochemistry (Mosc.)* **67,** 826–835.
13. Ponting, C. P., Hutton, M., Nyborg, A., Baker, M., Jansen, K. & Golde, T. E. (2002) *Hum. Mol. Genet*. **11,** 1037–1044.
14. Weihofen, A., Binns, K., Lemberg, M. K., Ashman, K. & Martoglio, B. (2002) *Science* **296,** 2215–2218.
15. Moliaka, Y. K., Grigorenko, A., Madera, D. & Rogaev, E. I. (2004) *FEBS Lett*. **557,** 185–192.
16. Lemberg, M. K., Bland, F. A., Weihofen, A., Braud, V. M. & Martoglio, B. (2001) *J. Immunol*. **167,** 6441–6446.
17. McLauchlan, J., Lemberg, M. K., Hope, G. & Martoglio, B. (2002) *EMBO J*. **21,** 3980–3988.
18. Brenner, S. (1974) *Genetics* **77,** 71–94.
19. Merris, M., Wadsworth, W. G., Khamrai, U., Bittman, R., Chitwood, D. J. & Lenard, J. (2003) *J. Lipid Res*. **44,** 172–181.
20. Rocheleau, C. E., Downs, W. D., Lin, R., Wittmann, C., Bei, Y., Cha, Y. H., Ali, M., Priess, J. R. & Mello, C. C. (1997) *Cell* **90,** 707–716.
21. Fire, A., Xu, S., Montgomery, M. K., Kostas, S. A., Driver, S. E. & Mello, C. C. (1998) *Nature* **391,** 806–811.
22. Timmons, L. & Fire, A. (1998) *Nature* **395,** 854.
23. Tabara, H., Hill, R. J., Mello, C. C., Priess, J. R. & Kohara, Y. (1999) *Development (Cambridge, U.K.)* **126,** 1–11.
24. Timmons, L., Court D. L. & Fire, A. (2001) *Gene* **263,** 103–112.
25. Mello, C. C., Kramer, J. M., Stinchcomb, D. & Ambros, V. (1991) *EMBO J*. **10,** 3959–3970.
26. Li, X. & Greenwald, I. (1996) *Neuron* **17,** 1015–1021.
27. Dewji, N. N. & Singer, S. J. (1997) *Proc. Natl. Acad. Sci. USA* **94,** 14025–14030.
28. Nyborg, A. C., Kornilova, A. Y., Jansen, K., Ladd, T. B., Wolfe, M. S. & Golde, T. E. (2004) *J. Biol. Chem*. **279,** 15153–15160.
29. Schroeter, E. H., Kisslinger, J. A. & Kopan, R. (1998) *Nature* **393,** 382–386.
30. Wolfe, M. S., Xia, W., Ostaszewski, B. L., Diehl, T. S., Kimberly, W. T. & Selkoe, D. J. (1999) *Nature* **398,** 513–517.
31. Priess, J. R., Schnabel, H. & Schnabel, R. (1987) *Cell* **51,** 601–611.
32. Doyle, T. G., Wen, C. & Greenwald, I. (2000) *Proc. Natl. Acad. Sci. USA* **97,** 7877–7881.
33. Yu, G., Nishimura, M., Arawaka, S., Levitan, D., Zhang, L., Tandon, A., Song, Y. Q., Rogaeva, E., Chen, F., Kawarai, T., *et al*. (2000) *Nature* **407,** 48–54.
34. Yochem, J., Tuck, S., Greenwald, I. & Han, M. (1999) *Development* **126,** 597–606.
35. Silberkang, M., Havel, C. M., Friend, D. S., McCarthy, B. J. & Watson, J. A. (1983) *J. Biol. Chem*. **258,** 8503–8511.
36. Bottjer, K. P., Weinstein, P. P. & Thompson, M. J. (1985) *Comp. Biochem. Physiol. B* **82,** 99–106.
37. Kurzchalia, T. V. & Ward, S. (2003) *Nat. Cell Biol*. **5,** 684–688.
38. Thummel, C. S. (1996) *Trends Genet*. **12,** 306–310.
39. Shim, Y. H., Chun, J. H., Lee, E. Y. & Paik, Y. K. (2002) *Mol. Reprod. Dev*. **61,** 358–366.
40. Jia, K., Albert, P. S. & Riddle, D. L. (2002) *Development (Cambridge, U.K.)* **129,** 221–231.
41. Kostrouchova, M., Krause, M., Kostrouch, Z. & Rall, J. E. (2001) *Proc. Natl. Acad. Sci. USA* **98,** 7360–7365.
42. Nitta, M., Ku, S., Brown, C., Okamoto, A. Y. & Shan, B. (1999) *Proc. Natl. Acad. Sci. USA* **96,** 6660–6665.
43. Gissendanner, C. R. & Sluder, A. E. (2000) *Dev. Biol*. **221,** 259–272.
44. Roggo, L., Bernard, V., Kovacs, A. L., Rose, A. M., Savoy, F., Zetka, M., Wymann, M. P. & Muller, F. (2002) *EMBO J*. **21,** 1673–1683.
45. Kamikura, D. M. & Cooper, J. A. (2003) *Genes Dev*. **17,** 2798–2811.
46. Selkoe D. & Kopan R. (2003) *Annu. Rev. Neuroscience*. **26,** 565–597.

Table 1. No rescue of *sel-12/lin-12, glp-1* defects by *Ce-imp-2* RNAi

Strains	RNAi	Total worms	T, ˚C	Phenotype
sel-12(ar171) unc-1	*Ce-imp-2*	136	room	100% Egl
unc-32(e189) lin-12(n676n930)III		147	25	100% Egl
glp-1(e2142ts)		P_0 , 162	25	F_1 , 100% Emb

No rescue of *sel-12/lin-12, glp-1* defects by *Ce-imp-2* RNAi. Deficiency in *sel-12* alone (with a functional *hop-1* paralogous gene) does not induce the *lin-12*, *glp-1* phenotypes, but certain alleles produce an incompletely (e.g., *sel-12 (ar131*)) or completely (e.g., *sel-12 (ar171*) *unc-1*) penetrant recessive egg-laying defective phenotype (Egl) and large vulval protrusion. The loss-of-function of certain *lin-12* mutants is also associated with the Egl (egg-laying defect) phenotype and abnormal vulval development. We found no prominent Egl phenotype or protruding vulvae in N2 wild-type animals fed with *Ce-imp-2* dsRNA. However, we occasionally observed eggs that hatched within the mother and reduced brood size, resembling effects in *sel-12* mutants (1). We next used sensitized genetic backgrounds to look for interactions between *Ce-imp-2* and Notch-pathway components. To do this, we used RNAi to knock down *Ce-imp-2* activity in (*i*) *sel-12(ar171)unc-1(e538)* and *sel-12(ar131)* (presenilin loss-of-function mutants); (*ii*) *unc-32(e189) lin-12(n676n930) III* strain (temperature sensitive hypomorphic *lin-12* allele at 25˚C); (*iii*) *lin-12(n137)/unc-32(e189)III;him-5(e1467)V* (a *lin-12* hypermorphic strain); (*iv*) *glp-1(e2142ts)* (temperature-sensitive hypomorphic *glp-1* allele). None of these mutant strains exhibited enhancement or suppression of their corresponding phenotypes upon induction *Ce-imp-2* (RNAi). For example, in the *sel-12(ar171) unc-1* and *sel-12(ar131)* mutant strain, RNAi targeting the *sel-12* homolog *hop-1* induces an embryonic arrest and loss of anterior pharynx (2). No such defect in pharyngeal development was induced by *Ce-imp-2* (RNAi) in the *sel-12* mutants background. We found also that *Ce-imp-2* (RNAi) did not rescue Egl phenotype of *sel-12(ar171) unc-1*. Likewise, inhibition of *Ce-imp-2* in the *lin-12(n137)/unc-32(e189)III;him-5(e1467)V* hypermorphic strain did not reduce or enhance the multivulva phenotype of this strain. Finally, RNAi targeting

Ce-imp-2 in the hypomorphic *glp-1(2142ts)* genetic background did not reduce the rate of embryonic lethality (Emb) in this strain.

1. Lakowski, B., Eimer, S., Gobel, C., Bottcher, A., Wagler, B. & Baumeister, R. (2003) *Development* **130,** 2117-2128.

2. Li, X. & Greenwald, I. (1997) *Proc. Natl. Acad. Sci. USA* **94,** 12204-12209.

Table 2. ISC phenotypes in N2 worms (P_0) fed with dsRNA *Ce-imp-2* or dsRNA *Ce-lrp-1*

Strain	RNAi	Total worms	ISC head	ICS tail	Body constrictions
N2	*Ce-imp-2*	999 (100%)	240 (24%)	19 (1.9%)	4 (0.4%)
N2	*Ce-lrp-1*	326 (100%)	46 (14.1%)	12 (3.7%)	21 (6.4%)

Supporting Text

Effect of *Ce-imp-2* RNAi on brood size. Because the reduced number of eggs in a common population may merely reflect increased death of worms during the molt stages, we examined the brood size of individual ST2 worms on *Ce-imp-2* RNAi food. The ST2 strain expressing GFP in the CNS was used for easier detection of weak and dead worms at the late embryonic and early L_1 stages. Synchronized L_1 larvae (n = 10) were placed in separate *Ce-imp-2* dsRNA plates. The hatched larvae and eggs were inspected daily during 5 days; each day, the parent worms were transferred to fresh plates. Worms that developed incomplete shedding of cuticle (ISC) at the L_4-adult stage died, some of them having a low number of progeny hatched inside dead mothers. The surviving worms were able to lay eggs over the next 2 or 3 days, but with a mean brood size at least 3-fold less than control RNAi worms. About 80% of these progeny died at the late embryonic-early larvae stages.

Supporting Materials and Methods

RNA Interference (RNAi) by Double-Stranded RNA (dsRNA) Feeding. To conduct RNAi by feeding, we have subcloned the full-length 1.54-kb cDNA *Ce-imp-2* (yk671a5 clone) into the L4440 vector. We also subcloned *Ce-imp-2* cDNA fragments that include the 1329-bp middle region, and nonoverlapping fragments [5'- *Ce-imp-2* sequence (485 bp) and 3'-*Ce-imp-2* sequences (823 bp)] into L4440 (Fig. 5*B*). We believed that application of the different dsRNAs would exclude theoretically possible nonspecific RNAi effects and might provide a more detailed characterization of *Ce-imp-2*-regulated phenotypes on different stages of worm development. Identical phenotype defects were induced by expression of all these RNAi constructs; these results were reproduced in multiple experiments in three laboratories (Brudnick Neuropsychiatric Research Institute, Howard Hughes Medical Institute, and Laboratory of Molecular Brain Genetics). Sub-fragments of *Ce-imp-2* cDNA for RNAi by feeding were cloned into L4440 vector using primers 5'- TTTTGAATTCGACGGCTAGCAATGTCACAG-3', 5'-TTTTCTCGAGTCCACATGTCT TGATTCATC-3' (1329 bp) ; 5'-TTTTGAATTC

CTTTCGCGACATGGCTGA-3', 5'-TTTTCTCGAGTATAAGCGTATGTAG CCGCATTT -3' (485 bp); and 5'-TTTTGAATTCCCATTTG TTACCGCGTTTCT-3', 5'-TTTTCTCGAG GCCGGAGTCTACTTTCTTTCG-3' (823 bp) (Fig. 5*B*). cDNA for *Ce-lrp-1* gene corresponding to the extracellular part of the protein was subcloned into *Bam*HI-*Xho*I L4440 using primers 5'-TTTTGGATCCGCCGTACTTGCTCTCCATTC-3' and 5'- TTTTCTCGAGCCATCCAATCGACATTTTCC-3' (Fig. 5*B*). These constructs were transferred to the *Escherichia coli* strain HT115. The bacterial cultures were grown in 1 liter of LB-Amp to $OD_{600} \approx 1$, spun down, and resuspended in 50 ml of LB , containing Amp 60 μg/ml and 7% DMSO, and were frozen and stored in 5-ml aliquots at -70°C. For each experiment, a fresh aliquot was used. For dsRNA induction, 100 μl of isopropyl β-D-thiogalactoside (IPTG) (200 mg/ml) was added to each *E.coli* stock. Synchronized population of worms was obtained by using the standard hypochlorite method. L_1 stage larvae, hatched in M9 buffer, were placed on dsRNA agarose plates, and the phenotype of worms (P_0) was analyzed on the second and third days at room temperature. On the third day, eggs were collected using the hypochlorite treatment. Eggs were placed on dsRNA plates, and the phenotype of F_1 progeny was analyzed for the next two days.

Mammalian Cell Lines and Western Blot Analysis. Cell lines with stable or transiently transfected constructs were maintained in appropriate media supplemented with 10% FBS (GIBCO/BRL); 1% penicillin/streptomycin, 2 mM L-glutamine at 37°C; and 5% CO_2. Human embryonic kidney (HEK) 293 cells and mouse fibroblasts were cultured in DMEM; PC12 rat pheochromocytoma cells in RPMI medium 1640; Chinese hamster ovary (CHO) cells in F12; and H4 (human neuroglioma) cells in Opti-MEM (GIBCO/BRL). Transfection was performed using LipofectAMINE PLUS Reagent (GIBCO/BRL). Twenty-four to 48 h after transfection, cells were briefly washed twice in cold PBS, lysed in modified RIPA buffer (50 mM Tris•HCl, pH 7.4/1% Nonidet P-40/0.25% sodium deoxycholate Na/150 mM NaCl/1 mM EDTA) supplemented with protease inhibitors (Roche Molecular Biochemicals) for 15 min at 4°C, and centrifuged at 20,800 × *g* for 10 min at 4°C. For coimmunoprecipitation (co-IP) experiments of hIMP1, HEK293 and H4 cells were cotransfected with hIMP1-c-myc and hIMP1-V5 plasmids.

Ten to 20 μg of protein extracts were mixed with SDS sample buffer (twice) (Invitrogen) containing reducing agent, centrifuged at 12,000 rpm for 5 min with or without prior boiling for 5 min, and loaded onto SDS polyacrylamide gel (PAAG) minigels. Prestained molecular weight marker was loaded into a separate well. Electrophoresis was run in 10–20% Tricine PAAG or 10% SDS PAAG for hIMP1 products and 8% Tris-Glycine SDS PAAG for NotchΔE and NOTCH1 intracellular domain (NICD) fragments in corresponding 1× SDS running buffer at 125 V. Electro-transfer onto poly(vinylidene difluoride) (PVDF) membranes was performed in a Tris-Glycine transfer buffer 12 mM Tris base, 96 mM glycine, 20% methanol. After transfer, membranes were washed in TBS-T buffer (50 mM Tris•HCl, pH 7.4/150 mM NaCl/0.05% Tween 20) three times for 5 min, incubated in blocking buffer (5% milk in TBS-T) at room temperature for 1 h, and hybridized with primary antibodies, 1:1,000–1:5,000 dilution in 10 ml of hybridization buffer (1% milk in TBS-T) at room temperature for 1 h, or 4°C overnight. The primary polyclonal and monoclonal antibodies against N-terminal-PS1 fragments and N-terminal hIMP1 or V5 and c-myc C-terminal targets of hIMP1 or Notch epitopes have been used to control efficiency of expression in each transfection experiment. After incubation with appropriate secondary antibodies, signal visualization was performed using ECL Western blotting detection reagent kit (Amersham Pharmacia) by exposure to an x-ray film.

Pulse-chase experiments. HEK293 cells were transfected with Notch, hIMP1, and PS1 constructs using LipofectAMINE PLUS Reagent (GIBCO/BRL). NotchΔE and NICD (obtained from R. Kopan, Washington University School of Medicine, St. Louis) were fused to c-myc epitopes. hIMP1 wild-type or mutant isoforms were cloned into cDNA3 or pcDNA4/c-myc-HisB. Twenty-four hours after transfection, cells were starved for 2 h in methionine and cysteine-free medium without serum, labeled with 0.1 mCi of [^{35}S]methionine and [^{35}S]cysteine for 30 min, chased for 1 h in DMEM medium supplemented with 10% FBS, and lysed in RIPA buffer with 1% Nonidet P-40 and protease inhibitor mixture. Protein extracts were immunoprecipitated with anti-c-myc-antibodies to Notch-C-terminal tag-epitopes and subjected to electrophoresis and autoradiography.

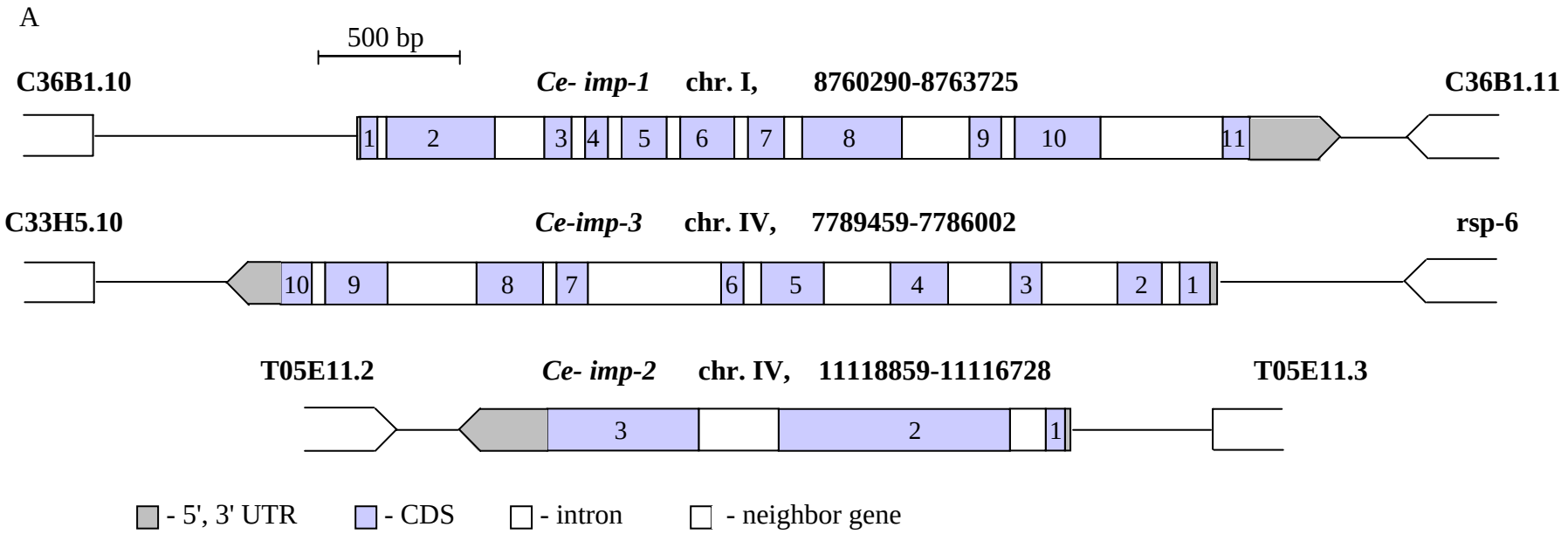
A
500 bp
C36B1.10
Ce- imp-1
chr. I,
8760290-8763725
C36B1.11
1
2
3
4
5
6
7
8
9
10
11
C33H5.10
Ce-imp-3
chr. IV,
7789459-7786002
rsp-6
10
9
8
7
6
5
4
3
2
1
T05E11.2
Ce- imp-2
chr. IV,
11118859-11116728
T05E11.3
3
2
1
- 5', 3' UTR
- CDS
- intron
- neighbor gene

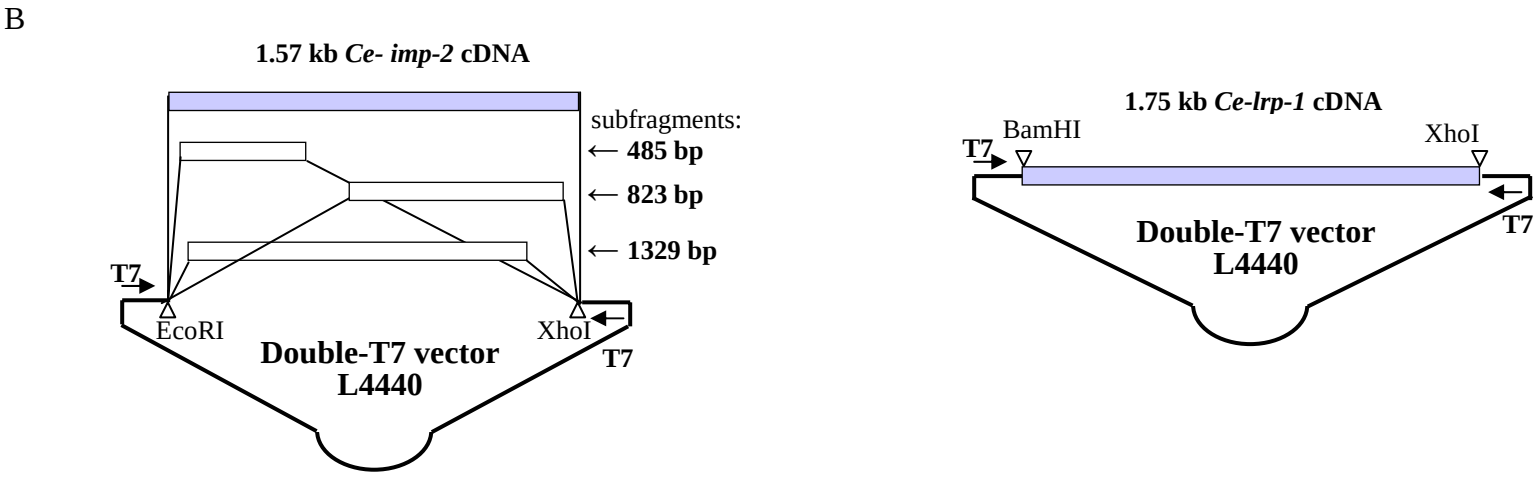
B
1.57 kb Ce- imp-2 cDNA
subfragments:
← 485 bp
← 823 bp
← 1329 bp
T7
EcoRI
XhoI
T7
Double-T7 vector
L4440
1.75 kb Ce-lrp-1 cDNA
BamHI
XhoI
T7
T7
Double-T7 vector
L4440

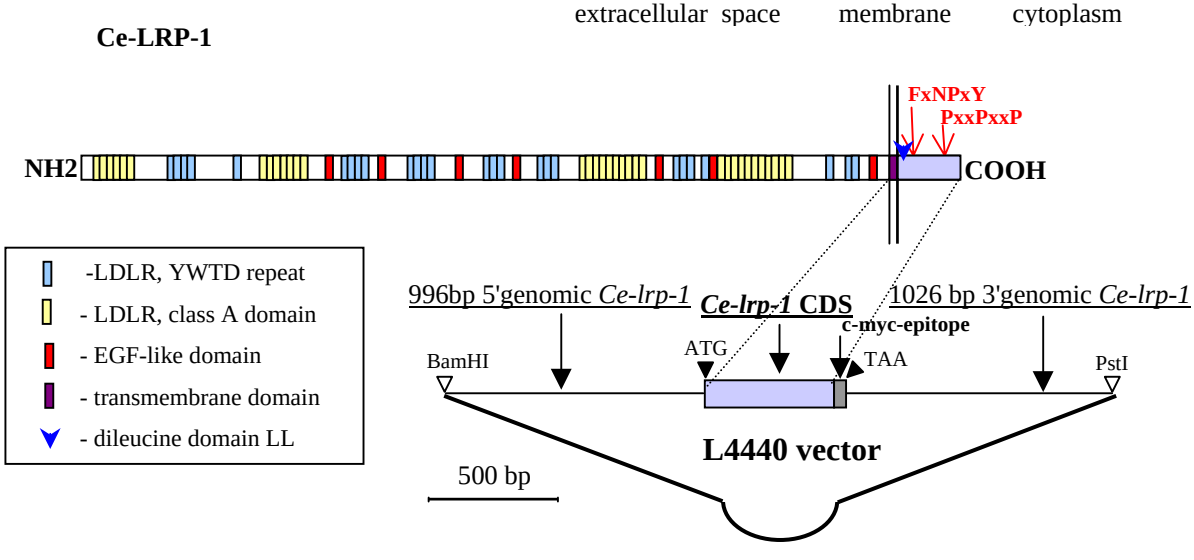
Ce-LRP-1
extracellular space
membrane
cytoplasm
FxNPxY
PxxPxxP
NH2
COOH
-LDLR, YWTD repeat
- LDLR, class A domain
- EGF-like domain
- transmembrane domain
- dileucine domain LL
996bp 5'genomic Ce-lrp-1
Ce-lrp-1 CDS
1026 bp 3'genomic Ce-lrp-1
c-myc-epitope
BamHI
ATG
TAA
PstI
L4440 vector
500 bp

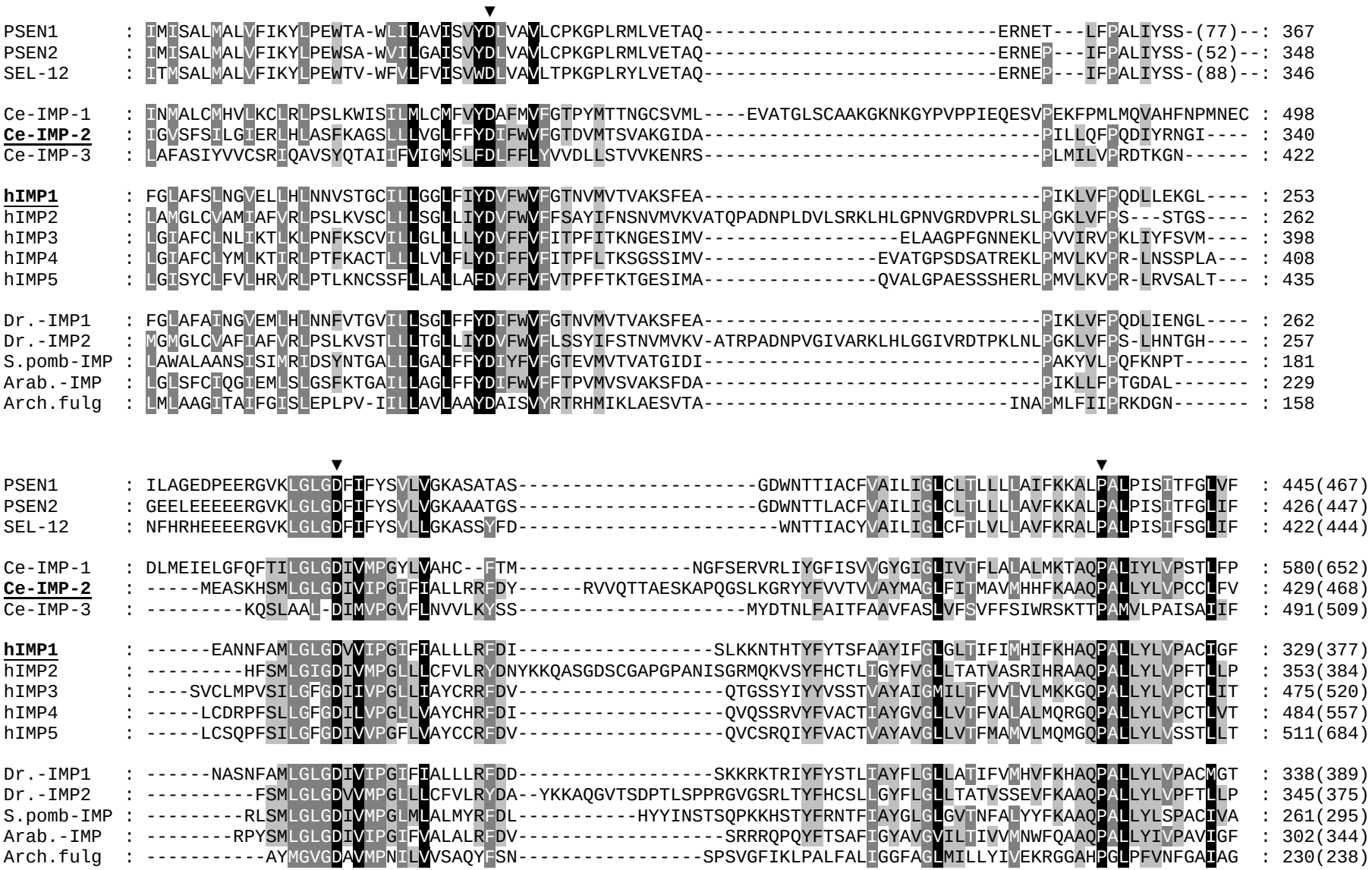
PSEN1 : IMISALMALVFIKYLPEWTA-WLILAVISVYDLVAVLCPKGPLRMLVETAQ----------ERNET---LFPALIYSS-(77)--: 367
PSEN2 : IMISALMALVFIKYLPEWSA-WVILGAISVYDLVAVLCPKGPLRMLVETAQ----------ERNEP---IFPALIYSS-(52)--: 348
SEL-12 : ITMSALMALVFIKYLPEWTV-WFVLFVISVWDLVAVLTPKGPLRYLVETAQ----------ERNEP---IFPALIYSS-(88)--: 346
Ce-IMP-1 : INMALCMHVLKCLRLPSLKWISILMLCMFVYDAFMVFGTPYMTTNGCSVML----EVATGLSCAAKGKNKGYPVPPIEQESVPEKFPMLMQVAHFNPMNEC : 498
Ce-IMP-2 : IGVSFSILGIERLHLASFKAGSLLLVGLFFYDIFWVFGTDVMTSVAKGIDA----------PILLQFPQDIYRNGI---- : 340
Ce-IMP-3 : LAFASIYVVCSRIQAVSYQTAIIFVIGMSLFDLFFLYVVDLLSTVVKENRS----------PLMILVPRDTKGN------ : 422
hIMP1 : FGLAFSLNGVELLHLNNVSTGCILLGGLFIYDVFWVFGTNVMVTVAKSFEA----------PIKLVFPQDLLEKGL---- : 253
hIMP2 : LAMGLCVAMIAFVRLPSLKVSCLLLSGLLIYDVFWVFFSAYIFNSNVMVKVATQPADNPLDVLSRKLHLGPNVGRDVPRLSLPGKLVFPS---STGS---- : 262
hIMP3 : LGIAFCLNLIKTLKLPNFKSCVILLGLLLLYDVFFVFITPFITKNGESIMV----------ELAAGPFGNNEKLPVVIRVPKLIYFSVM---- : 398
hIMP4 : LGIAFCLYMLKTIRLPTFKACTLLLLVLFLYDIFFVFITPFLTKSGSSIMV----------EVATGPSDSATREKLPMVLKVPR-LNSSPLA--- : 408
hIMP5 : LGISYCLFVLHRVRLPTLKNCSSFLLALLAFDVFFVFVTPFFTKTGESIMA----------QVALGPAESSSHERLPMVLKVPR-LRVSALT--- : 435
Dr.-IMP1 : FGLAFATNGVEMLHLNNFVTGVILLSGLFFYDIFWVFGTNVMVTVAKSFEA----------PIKLVFPQDLIENGL---- : 262
Dr.-IMP2 : MGMGLCVAFIAFVRLPSLKVSTLLLTGLLIYDVFWVFLSSYIFSTNVMVKV-ATRPADNPVGIVARKLHLGGIVRDTPKLNLPGKLVFPS-LHNTGH---- : 257
S.pomb-IMP : LAWALAANSISIMRIDSYNTGALLLGALFFYDIYFVFGTEVMVTVATGIDI----------PAKYVLPQFKNPT------ : 181
Arab.-IMP : LGLSFCIQGIEMLSLGSFKTGAILLAGLFFYDIFWVFFTPVMVSVAKSFDA----------PIKLLFPTGDAL------- : 229
Arch.fulg : LMLAAGITAIFGISLEPLPV-IILLAVLAAYDAISVYRTRHMIKLAESVTA----------INAPMLFIIPRKDGN------- : 158
PSEN1 : ILAGEDPEERGVKLGLGDFIFYSVLVGKASATAS----------GDWNTTIACFVAILIGLCLTLLLLAIFKKALPALPISITFGLVF : 445(467)
PSEN2 : GEELEEEEERGVKLGLGDFIFYSVLVGKAAATGS----------GDWNTTLACFVAILIGLCLTLLLLAVFKKALPALPISITFGLIF : 426(447)
SEL-12 : NFHRHEEEERGVKLGLGDFIFYSVLLGKASSYFD----------WNTTIACYVAILIGLCFTLVLLAVFKRALPALPISIFSGLIF : 422(444)
Ce-IMP-1 : DLMEIELGFQFTILGLGDIVMPGYLVAHC--FTM----------NGFSERVRLIYGFISVVGYGIGLIVTFLALALMKTAQPALIYLVPSTLFP : 580(652)
Ce-IMP-2 : -----MEASKHSMLGLGDIVIPGIFIALLRRFDY------RVVQTTAESKAPQGSLKGRYYFVVTVVAYMAGLFITMAVMHHFKAAQPALLYLVPCCLFV : 429(468)
Ce-IMP-3 : ---------KQSLAAL-DIMVPGVFLNVVLKYSS----------MYDTNLFAITFAAVFASLVFSVFFSIWRSKTTPAMVLPAISAIIF : 491(509)
hIMP1 : ------EANNFAMLGLGDVVIPGIFIALLLRFDI----------SLKKNTHTYFYTSFAAYIFGLGLTIFIMHIFKHAQPALLYLVPACIGF : 329(377)
hIMP2 : ---------HFSMLGIGDIVMPGLLLCFVLRYDNYKKQASGDSCGAPGPANISGRMQKVSYFHCTLIGYFVGLLTATVASRIHRAAQPALLYLVPFTLLP : 353(384)
hIMP3 : ----SVCLMPVSILGFGDIIVPGLLIAYCRRFDV----------QTGSSYIYYVSSTVAYAIGMILTFVVLVLMKKGQPALLYLVPCTLIT : 475(520)
hIMP4 : -----LCDRPFSLLGFGDILVPGLLVAYCHRFDI----------QVQSSRVYFVACTIAYGVGLLVTFVALALMQRGQPALLYLVPCTLVT : 484(557)
hIMP5 : -----LCSQPFSILGFGDIVVPGFLVAYCCRFDV----------QVCSRQIYFVACTVAYAVGLLVTFMAMVLMQMGQPALLYLVSSTLLT : 511(684)
Dr.-IMP1 : ------NASNFAMLGLGDIVIPGIFIALLLRFDD----------SKKRKTRIYFYSTLIAYFLGLLATIFVMHVFKHAQPALLYLVPACMGT : 338(389)
Dr.-IMP2 : ----------FSMLGLGDVVMPGLLLCFVLRYDA--YKKAQGVTSDPTLSPPRGVGSRLTYFHCSLLGYFLGLLTATVSSEVFKAAQPALLYLVPFTLLP : 345(375)
S.pomb-IMP : ---------RLSMLGLGDIVMPGLMLALMYRFDL----------HYYINSTSQPKKHSTYFRNTFIAYGLGLGVTNFALYYFKAAQPALLYLSPACIVA : 261(295)
Arab.-IMP : --------RPYSMLGLGDIVIPGIFVALALRFDV----------SRRRQPQYFTSAFIGYAVGVILTIVVMNWFQAAQPALLYIVPAVIGF : 302(344)
Arch.fulg : -----------AYMGVGDAVMPNILVVSAQYFSN----------SPSVGFIKLPALFALIGGFAGLMILLYIVEKRGGAHPGLPFVNFGAIAG : 230(238)

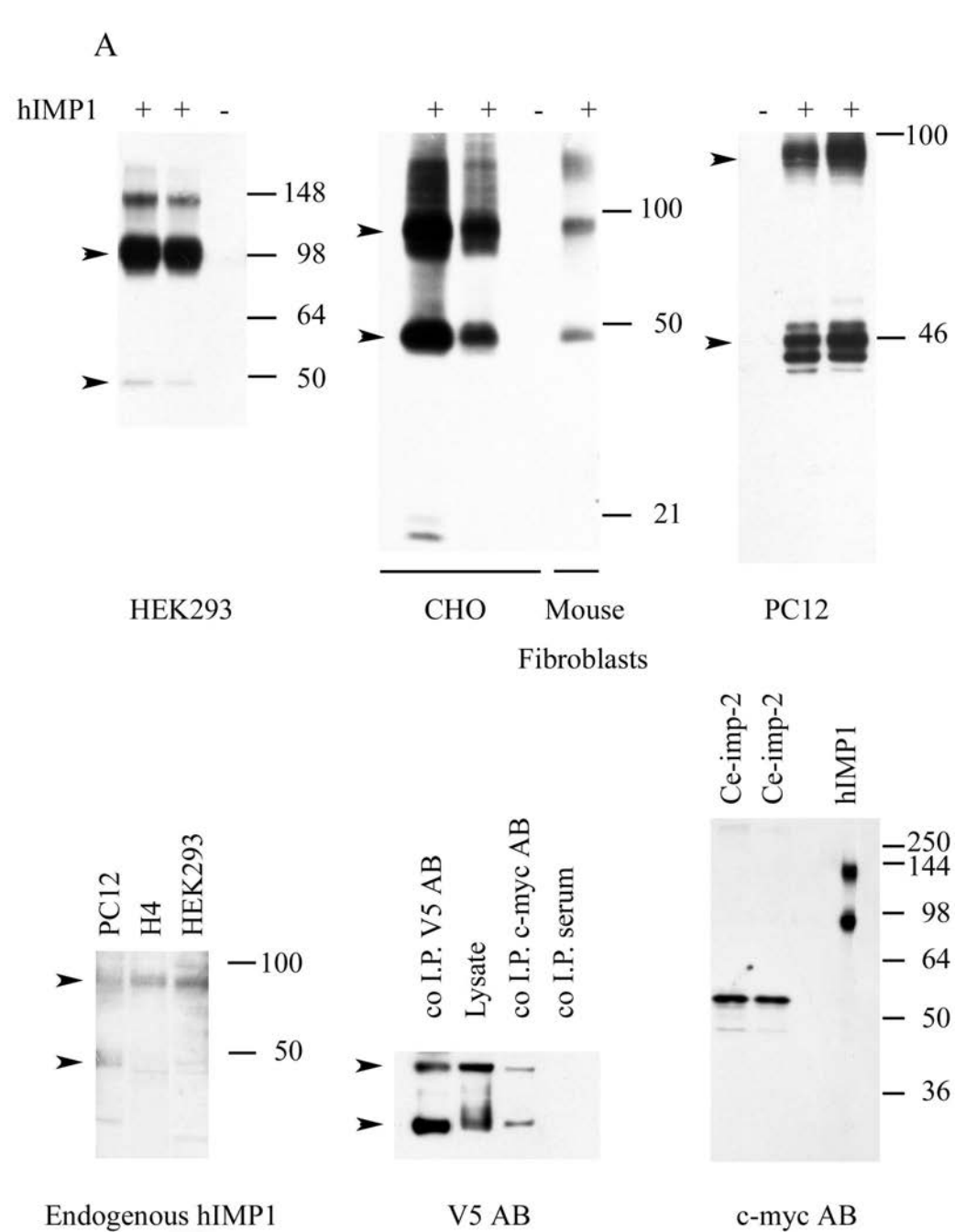
A
hIMP1
+ + -
148
98
64
50
+ + - +
100
50
21
- + +
100
46
HEK293
CHO
Mouse Fibroblasts
PC12
PC12
H4
HEK293
100
50
co I.P. V5 AB
Lysate
co I.P. c-myc AB
co I.P. serum
Ce-imp-2
Ce-imp-2
hIMP1
250
144
98
64
50
36
Endogenous hIMP1
V5 AB
c-myc AB

B

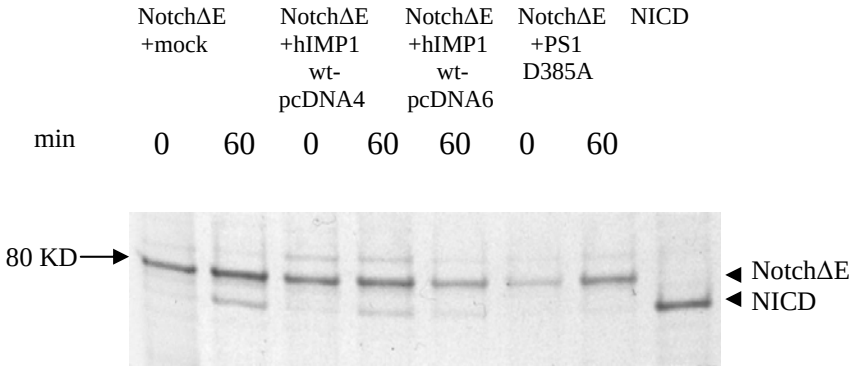
NotchΔE +mock
NotchΔE +hIMP1 wt-pcDNA4
NotchΔE +hIMP1 wt-pcDNA6
NotchΔE +PS1 D385A
NICD
min
0
60
0
60
60
0
60
80 KD
NotchΔE
NICD

C

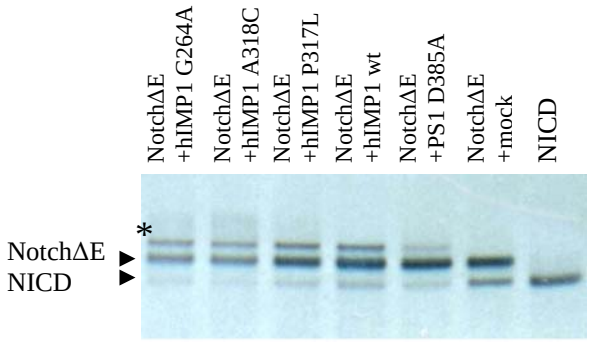
NotchΔE +hIMP1 G264A
NotchΔE +hIMP1 A318C
NotchΔE +hIMP1 P317L
NotchΔE +hIMP1 wt
NotchΔE +PS1 D385A
NotchΔE +mock
NICD
*
NotchΔE
NICD

D

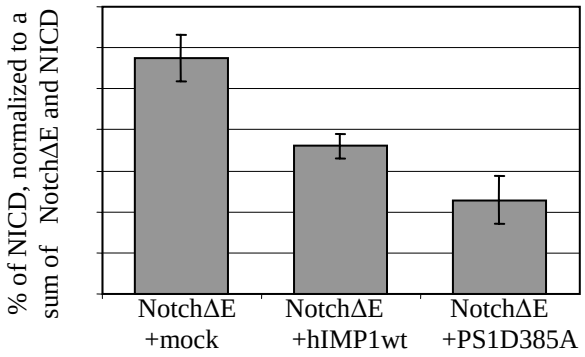
% of NICD, normalized to a sum of NotchΔE and NICD
NotchΔE +mock
NotchΔE +hIMP1wt
NotchΔE +PS1D385A

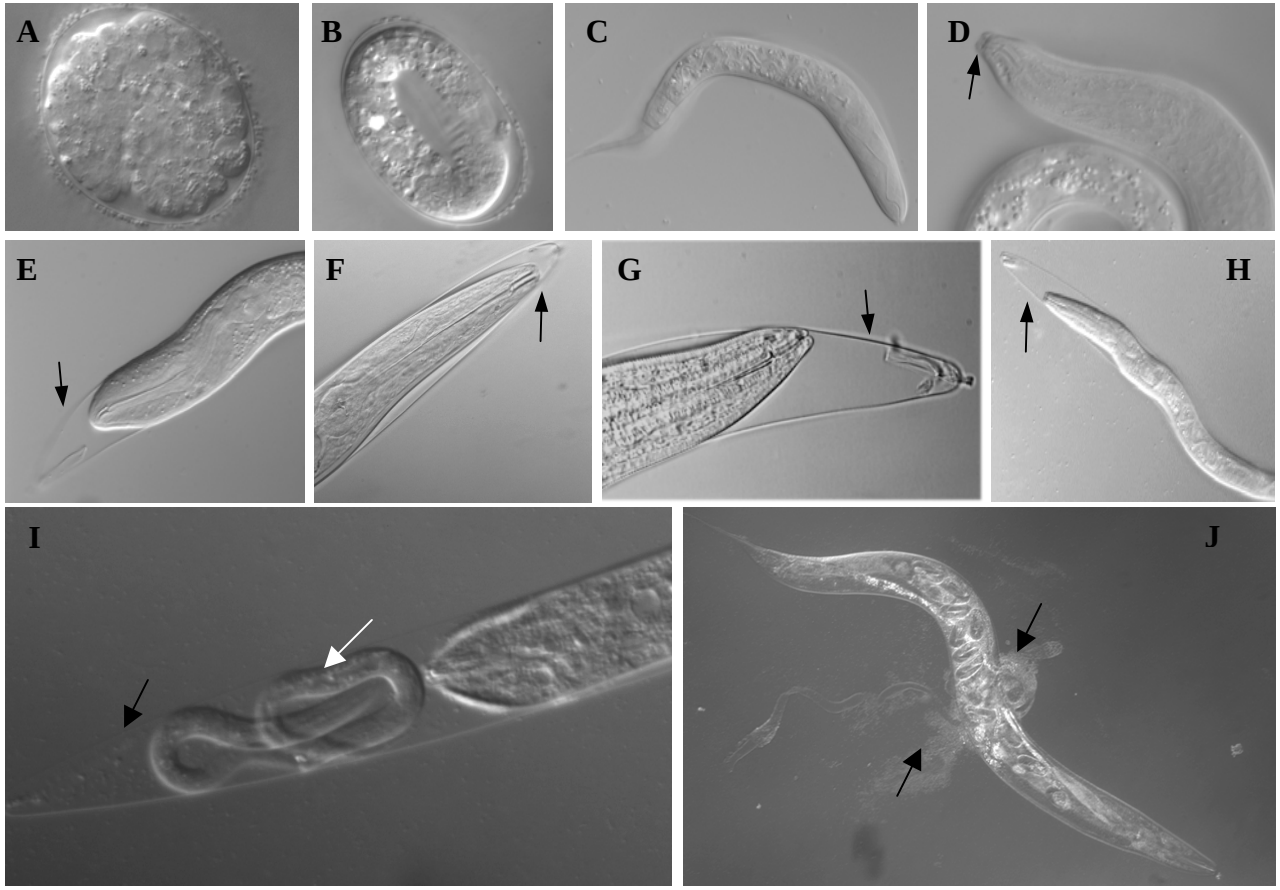
A
B
C
D
E
F
G
H
I
J

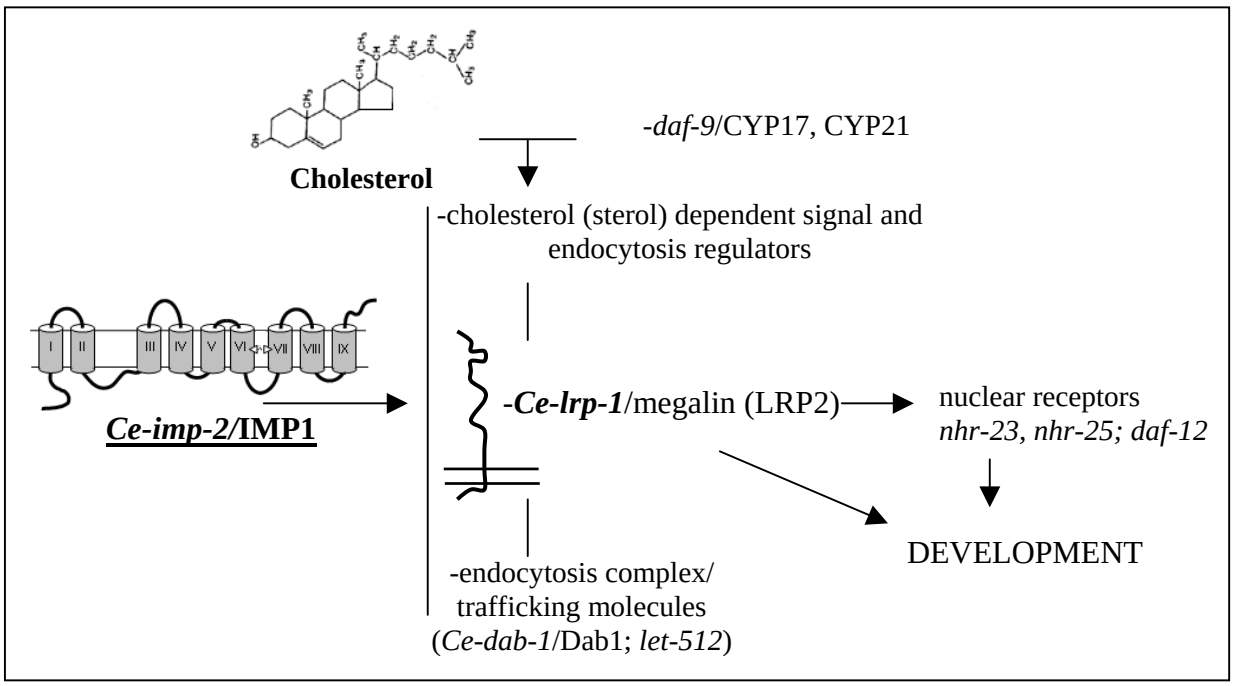
Cholesterol
-daf-9/CYP17, CYP21
-cholesterol (sterol) dependent signal and endocytosis regulators
I
II
III
IV
V
VI
VII
VIII
IX
Ce-imp-2/IMP1
-Ce-lrp-1/megalin (LRP2)
nuclear receptors
nhr-23, nhr-25; daf-12
DEVELOPMENT
-endocytosis complex/ trafficking molecules
(Ce-dab-1/Dab1; let-512)